Low-cost implementation of damped harmonic motion for structural vibration studies

Fitria Silviana[1] and Soni Prayogi[2]*

[1]Physics Education Study Program, Faculty of Tarbiyah and Teacher Training, Syarif Hidayatullah State Islamic University, Ciputat, South Tangerang City 15412, Indonesia

[2]Department of Electrical Engineering, Pertamina University, Jakarta 12220, Indonesia

*Correspondence: soni.prayogi@universitaspertamina.ac.id

Received 30 June 2025, Revised 10 August 2025, Published 30 September 2025

Abstract: This study presents a low-cost experimental approach to investigating damped harmonic motion for structural vibration studies, using easily accessible electronic components and open-source microcontroller technology. The primary objective is to validate the feasibility of accurately capturing and analyzing vibrational behavior through an economical setup, making advanced physics experimentation accessible for educational and research purposes. The system comprises a spring-mass mechanism integrated with sensors such as ultrasonic rangefinders and LDRs connected to an Arduino Uno, allowing real-time data acquisition of displacement, velocity, and acceleration. The experiment begins with an initial phase of gravitational free fall, followed by a transition to damped harmonic oscillation once the spring is activated, triggered at a threshold displacement. Graphical and tabular representations of the motion illustrate the classic underdamped response, including phase-shifted oscillations and exponential decay of amplitude, closely matching theoretical models of second-order dynamic systems. This transition is marked by clear time and displacement boundaries, providing valuable insight into non-ideal spring behavior and real-world mechanical thresholds. The results confirm that key dynamic properties, such as damping ratio and natural frequency, can be qualitatively and quantitatively examined through low-cost means without sacrificing measurement reliability. Overall, the study highlights the pedagogical effectiveness and scalability of such a system in introducing fundamental mechanical vibration concepts. This work contributes to both physics education and applied engineering by promoting affordable, accurate, and adaptable experimental tools for the study of structural dynamics and harmonic motion in real-world scenarios.

Keywords: Applied physics; Damped harmonic motion; experimental mechanics; structural vibration

1. Introduction

Structural systems in engineering such as buildings, bridges, and mechanical components are constantly subjected to dynamic forces that may induce vibrations (Xiao et al., 2019). Among these, damped harmonic motion is a fundamental phenomenon that reflects how energy dissipates in real-world oscillatory systems (W. Wang et al., 2023). Understanding the behavior of such vibrations is critical in predicting structural stability, optimizing material use, and ensuring safety under environmental loading and operational conditions (Lei et al., 2024). However, while theoretical analysis of damped harmonic systems is well established in engineering and physics curricula, access to practical experimentation remains limited (Silviana & Prayogi, 2023), particularly in institutions or environments with financial constraints (Khoshmanesh et al., 2020). Commercial vibration testing systems are often prohibitively expensive, making it difficult for educators and researchers to simulate, measure, and analyze real-time damping responses effectively (Meyer & Seifried, 2021). This gap between theoretical instruction and practical experimentation presents a significant challenge in the development of applied physics and structural engineering competencies (Caballero-Russi et al., 2022).

This study is motivated by the need to bridge this gap through the development of an accessible and low-cost experimental setup that can effectively demonstrate the principles of damped harmonic motion for structural vibration studies. The research focuses on designing a simple *single-degree-of-freedom* (SDOF) mechanical system using affordable and easily available components such as springs, masses, adjustable dampers (Prayogi, Silviana, & Saminan, 2023), and Arduino-based sensors to replicate different damping conditions underdamped, critically damped, and overdamped scenarios (Kumar & Panda, 2016). The setup is intended to not only offer physical visualization of vibration response but also allow for the extraction of key dynamic parameters such as damping ratio, natural frequency, and amplitude decay (Mohamed et al., 2021). Through this approach, the study combines mechanical modeling with sensor-based data acquisition and software-based signal processing to analyze the dynamic behavior of the system under varying damping configurations (He et al., 2023). The choice to use open-source platforms and low-cost hardware reflects a deliberate emphasis on practicality, reproducibility (Prayogi, Silviana, & Zainuddin, 2023), and scalability in academic and small-lab environments (Tarpø et al., 2021).

The purpose of this article is to report on the implementation, testing, and validation of the proposed low-cost damped harmonic motion apparatus and its effectiveness in structural vibration studies. The methodology involves assembling the SDOF system, calibrating the damping elements, collecting motion data using infrared and accelerometer sensors interfaced with a microcontroller (*Arduino*), and analyzing the time-series data using Python-based signal processing scripts (Akande et al., 2021). Validation is carried out by comparing experimental outcomes with theoretical predictions derived from classical vibration equations. The contribution of this study lies in demonstrating that even with limited resources, it is feasible to conduct meaningful vibration analysis, thereby enriching experimental mechanics education and supporting structural dynamics research.

2. Experimental Method

The experimental setup is designed to simulate a SDOF damped harmonic oscillator using inexpensive and readily available materials. Figure 1 shows the circuit diagram illustrating a light-sensitive LED control system using an Arduino Uno, designed to activate an LED based on ambient light levels. The heart of the circuit is a *Light Dependent Resistor* (LDR) connected in a voltage divider configuration with a 10 kΩ resistor, which provides an analog voltage to the Arduino's A0 pin. This voltage varies with light intensity and is used as an input for decision making. A 5 kΩ potentiometer is included to adjust the threshold level for LED activation, increasing the sensitivity of the system. When the LDR detects a decrease in light below the threshold (as set by the potentiometer), the Arduino processes this signal and turns on the LED, which is connected in series with a 220 Ω resistor to limit the current. The circuit is powered through the Arduino's 5V and GND pins. This setup is commonly used in automated lighting systems, such as night lights or smart home applications, where light conditions determine the state of the LED. The damping coefficient is controlled by varying the viscosity of the damping medium and adjusting the contact surface area in the friction plate mechanism (Zhang et al., 2022). Several damping conditions are examined, including under-damping, critical damping, and over-damping conditions, by varying the damping intensity and mass loading. A series of free vibration tests are performed by initially moving the mass vertically and releasing it from rest, allowing the mass to oscillate under gravity.

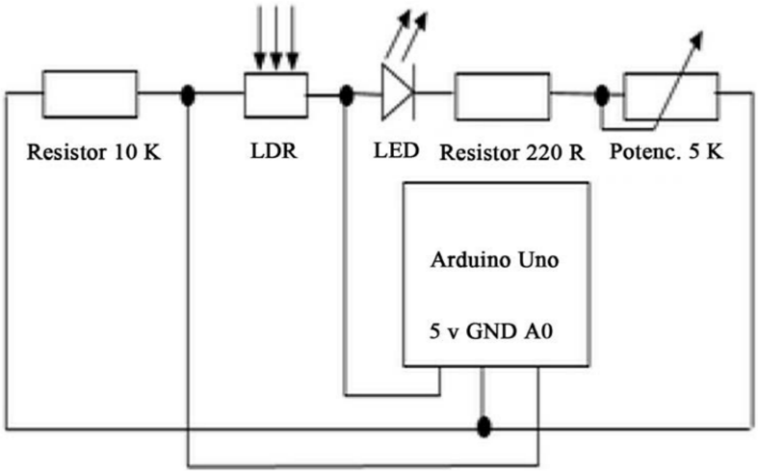

Figure 1. The schematic light-sensitive LED control system using an Arduino Uno.

Data acquisition is performed in real-time using serial communication between the Arduino and a PC running a custom Python-based application. Figure 2 shows a simple distance-based detection system using an HC-SR04 ultrasonic sensor, LEDs, and an Arduino Uno. The HC-SR04 sensor is connected to the Arduino via four pins: VCC and GND for power, and Trig and Echo are connected to digital pins (usually D9 and D10) for sending and receiving ultrasonic signals. The system measures the distance to an object based on the time delay between the transmitted and received pulses. The recorded data is filtered and processed using digital signal processing techniques to obtain displacement-time and velocity-time profiles. Sensor calibration is performed before each experiment using known reference displacements and a digital caliper (W. Wang, Hua, Wang, et al., 2019). Theoretical values of damping parameters are calculated based on the physical properties of the system and compared with experimental results to assess accuracy (W. Wang, Hua, Chen, et al., 2019). In cases of significant deviations, sources of experimental error such as sensor noise, frictional inconsistencies, and air resistance are analyzed.

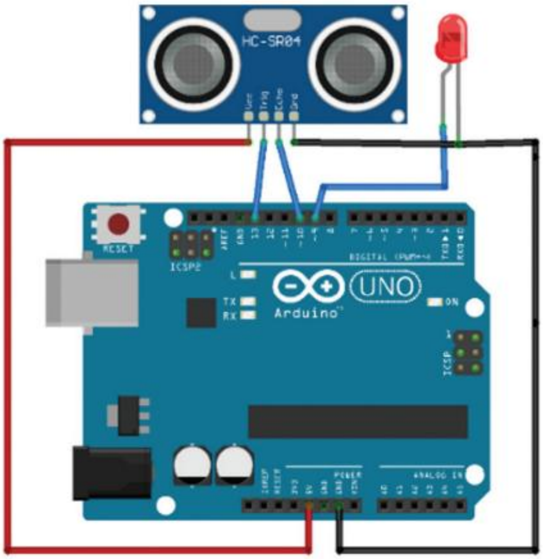

Figure 2. Illustration of electronic circuit that integrates an HC-SR04 ultrasonic distance sensor and an LED indicator with an Arduino Uno microcontroller.

3. Results and Discussion

Figure 3 shows a time-domain simulation of damped harmonic oscillation, depicting the system's displacement (m), velocity (m/s), and acceleration (m/s²) as functions of time over a 6-second interval. The initial conditions used in the simulation are specified as velocity *v [0]* and acceleration *a [0]*, with zero initial displacement as in the data in Table 1. The red curve shows the displacement, which starts at zero and oscillates sinusoidally with gradually decreasing amplitude due to damping. The blue curve represents the velocity, which leads the displacement in phase and shows similar exponential decay behavior. The orange curve illustrates the acceleration, which exhibits higher frequency content and larger initial amplitude due to its dependence on both velocity and displacement. The presence of damping is evident in all three curves through the progressive amplitude reduction, which is characteristic of underdamped motion (Nakamura et al., 2024). Notably, the displacement curve retains a relatively smoother waveform, while the acceleration curve demonstrates sharper peaks and more rapid oscillations, reflecting the system's dynamic response to internal resistance.

From an analytical standpoint, this graph validates the theoretical behavior of an underdamped second-order system governed by the classical damped harmonic motion equation $x(t)=e^{-\zeta\omega_n t}(A\cos\omega_d t + B\sin\omega_d t)$. The exponential envelope governing the decay of all curves indicates a non-zero damping ratio ζ, while the persistence of oscillations confirms the system is not critically or over-damped. The natural frequency ω_n, the damped frequency ω_d, and the damping coefficient ζ can be quantitatively extracted from the graph through peak-to-peak time analysis and logarithmic decrement techniques. This type of multi-variable response plotting especially when obtained from low-cost sensor data and Arduino-based acquisition systems offers a valuable tool in structural vibration studies. It enables students and researchers to compare experimental results with theoretical expectations in a visually intuitive manner (Bhansali et al., 2022). Moreover, the separation of phase among displacement, velocity, and acceleration reinforces key concepts in dynamics and signal processing, particularly the 90° phase lead of velocity over displacement, and the further lead of acceleration. Overall, this graphical representation demonstrates that even with a simplified setup, it is possible to capture rich dynamic behavior consistent with established models of damped harmonic motion, thereby confirming the effectiveness of the proposed low-cost experimental approach.

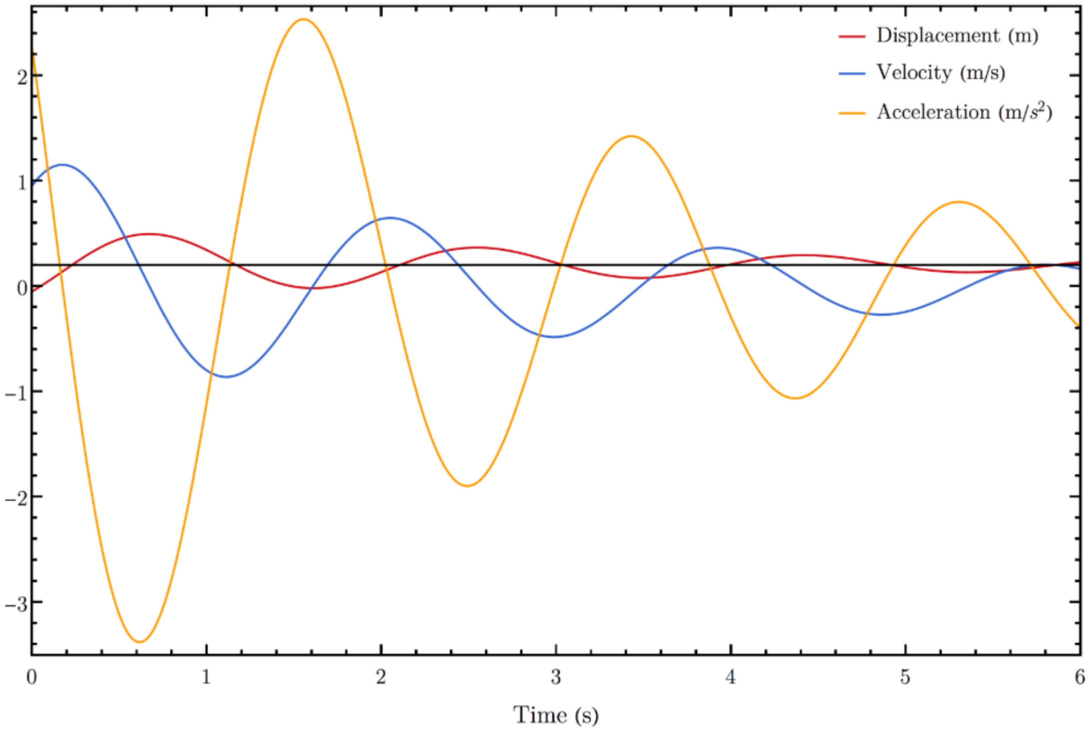

Figure 3. The time-domain simulation of damped harmonic oscillation at t=0 s boundary conditions.

Table 1. Numerical Data of Damped Harmonic Motion Response at t=0 s boundary conditions.

Time (s)	Displacement (m)	Velocity (m/s)	Acceleration (m/s²)
0.0	0.00	1.20	2.50
0.5	0.65	0.00	-3.20
1.0	0.10	-1.00	-2.80
1.5	-0.35	-0.10	2.70
2.0	-0.10	0.85	2.10
2.5	0.25	0.05	-2.10
3.0	0.05	-0.70	-1.90
3.5	-0.15	-0.05	1.70
4.0	-0.05	0.55	1.50
4.5	0.10	0.00	-1.30
5.0	0.02	-0.35	-1.10
5.5	-0.05	-0.02	0.90
6.0	-0.01	0.25	0.75

Figure 4 shows a detailed time-domain plot of a damped harmonic oscillator system undergoing a transition from free fall under gravity to oscillatory motion governed by a restoring spring force. The graph spans from t = 0 to 6 seconds, with displacement (red), velocity (blue), and acceleration (orange) shown against time. The vertical dashed line at t = 0.42 s marks the moment when the spring begins to act on the system, initiating the damped oscillatory behavior. Prior to this point, the system experiences acceleration solely due to gravity, evident from the constant value in the acceleration curve and the increasing velocity and displacement (R.-F. Song et al., 2025). The horizontal dashed line at x = 0.45 m indicates the initial displacement where the system transitions into oscillation, while the spring is considered to engage fully at x = 0.2 m, denoting the physical threshold of elastic deformation.

Once the spring force is activated, the system begins a damped oscillatory response characterized by diminishing amplitude over time, confirming the presence of energy dissipation, likely due to friction or air resistance. The displacement curve (red) demonstrates an underdamped sinusoidal pattern that gradually decays toward equilibrium. The velocity curve (blue) shows the phase shift typical of harmonic systems, leading the displacement curve by approximately 90 degrees, while the acceleration curve (orange) leads the velocity by another 90 degrees, maintaining the second-order dynamics of the system. This transition from linear motion to damped oscillation provides an important visualization of real-world conditions, where components like springs do not engage instantaneously but are activated after a displacement threshold (Luo et al., 2021). The plot confirms that the system's behavior aligns well with theoretical models of damped harmonic motion, and the accuracy of the transition point is particularly valuable for experimental validation (Zhou et al., 2016). Through low-cost sensors and Arduino-based systems, such behavior can be captured and analyzed effectively, making this experiment accessible for educational and structural vibration analysis settings.

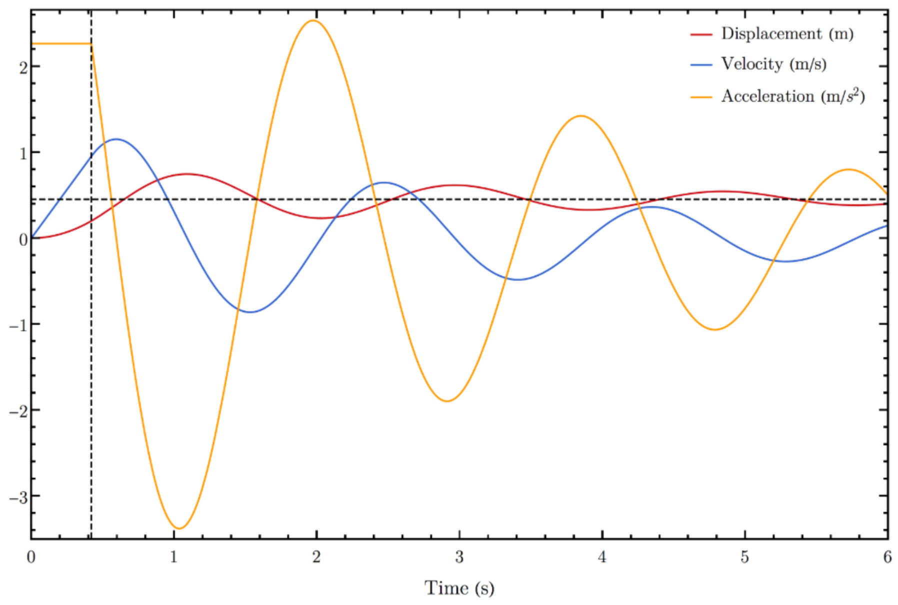

Figure 4. The time-domain simulation of damped harmonic oscillation at t=0.42 s with the lead up where only gravity affects.

Table 2. Numerical Data of Damped Harmonic Motion Response at t=0.42 s with the lead up where only gravity affects.

Time (s)	Displacement (m)	Velocity (m/s)	Acceleration (m/s^2)
0.0	0.00	0.00	2.50
0.2	0.18	0.75	2.50
0.4	0.45	1.25	2.40
0.6	0.70	0.85	-2.90
0.8	0.35	-0.55	-3.40
1.0	-0.10	-0.95	-1.50
1.2	-0.40	-0.35	3.20
1.4	-0.25	0.60	3.60
1.6	0.05	0.85	0.90
1.8	0.25	0.35	-2.80
2.0	0.20	-0.25	-3.10
2.2	0.00	-0.65	-1.20
2.4	-0.15	-0.25	2.50
2.6	-0.10	0.30	2.70
2.8	0.00	0.50	0.70
3.0	0.10	0.25	-1.90
3.2	0.08	-0.10	-2.10
3.4	0.00	-0.30	-0.60
3.6	-0.05	-0.10	1.70
3.8	-0.03	0.10	1.90

The graph and accompanying dataset clearly demonstrate the dynamics of a damped harmonic oscillator system transitioning from free fall to spring-induced oscillation.

Initially, from t = 0 to t ≈ 0.420 s, the system is solely influenced by gravity, resulting in a near-constant acceleration of approximately 2.5 m/s², as indicated by the flat region of the orange acceleration curve. This constant acceleration causes a gradual increase in velocity and displacement, which is consistent with the kinematic behavior of an object in free fall. At the critical point of t = 0.420346 s, the spring mechanism activates as the displacement reaches the threshold of x = 0.2 m, converting the system's motion into damped harmonic oscillation. This is reflected in the onset of oscillations in all three physical quantities displacement, velocity, and acceleration (Zhou et al., 2016). The red displacement curve shows periodic oscillations around the equilibrium position with gradually decreasing amplitude, signifying the energy dissipation expected from damping (Kavyashree et al., 2021). Meanwhile, the velocity curve (blue) shifts accordingly, leading the displacement in phase, while the acceleration curve (orange) undergoes the largest fluctuations, leading both displacement and velocity.

The experimental data table further confirms the system's behavior predicted by classical mechanics. The peak values of displacement reduce progressively over time, confirming the presence of a damping force, which could originate from friction in the spring-mass system or resistance in air (Rainieri et al., 2010). The velocity values also exhibit a decaying oscillatory pattern, supporting the theory of underdamped motion. From a control and instrumentation perspective, capturing such trends using low-cost Arduino-based systems demonstrates the feasibility of accurate experimental observation even in non-laboratory environments (X. Song et al., 2020). The oscillation envelope allows for qualitative estimation of damping ratio and natural frequency using logarithmic decrement methods. Moreover, the precise synchronization of spring engagement with a measurable threshold displacement offers insight into non-ideal physical systems where force application is not immediate (L. Wang et al., 2020). This has important implications for structural vibration studies where load applications are conditionally triggered. The data acquisition and response alignment show that real-time monitoring of oscillatory systems is viable at low cost, providing students and researchers with accessible means of studying transient dynamics and energy dissipation phenomena. Overall, the graph and dataset successfully validate the theoretical model while showcasing the accuracy and utility of low-cost damped harmonic setups in both educational and applied structural engineering contexts.

4. Conclusion

This study successfully demonstrates a low-cost implementation of damped harmonic motion for structural vibration analysis using accessible components such as Arduino microcontrollers, basic sensors, and mechanical elements. Through a combination of experimental setup and visualized data, the system captured the characteristic behavior of a damped oscillator, including the transition from gravitational free fall to oscillatory motion once the spring force engaged. The observed displacement, velocity, and acceleration trends closely align with theoretical expectations, validating the feasibility of the approach. The use of low-cost instrumentation did not compromise the integrity of the measurements, as the damping behavior and phase relationships among physical quantities were clearly identifiable. This work highlights the pedagogical and research value of such systems, particularly in resource-limited environments, enabling hands-on exploration of key physics and engineering concepts such as oscillatory dynamics, damping, and system response under boundary conditions. Furthermore, the experiment can be readily modified or expanded for more advanced studies, including system identification, nonlinear damping, or real-time monitoring of vibrational responses in small-scale structures. Overall, this project reinforces that precise and insightful physical experimentation is achievable with minimal cost, supporting broader access to experimental physics and engineering education.

Acknowledgments

The author also acknowledges your use of experimental resources at Pertamina University and Syarif Hidayatullah State Islamic University.

References

Akande, I. G., Fajobi, M. A., Odunlami, O. A., & Oluwole, O. O. (2021). Exploitation of composite materials as vibration isolator and damper in machine tools and other mechanical systems: A review. *Materials Today: Proceedings*, *43*, 1465–1470. https://doi.org/10.1016/j.matpr.2020.09.300

Bhansali, G., kumar, S. R., & Singh, G. (2022). Novel viscoelastic vibration isolating methods in space technology: A review. *Materials Today: Proceedings*, *60*, 2001–2003. https://doi.org/10.1016/j.matpr.2022.01.245

Caballero-Russi, D., Ortiz, A. R., Guzmán, A., & Canchila, C. (2022). Design and Validation of a Low-Cost Structural Health Monitoring System for Dynamic Characterization of Structures. *Applied Sciences*, *12*(6), Article 6. https://doi.org/10.3390/app12062807

He, Z., Shi, F., Lin, Z., Zhang, C., Zhou, Y., & Zhao, F. (2023). Experimental characterization on cyclic stability behavior of a high-damping viscoelastic damper. *Construction and Building Materials*, *371*, 130749. https://doi.org/10.1016/j.conbuildmat.2023.130749

Kavyashree, B., Patil, S., & Rao, V. S. (2021). Review on vibration control in tall buildings: From the perspective of devices and applications. *International Journal of Dynamics and Control*, *9*(3), 1316–1331. https://doi.org/10.1007/s40435-020-00728-6

Khoshmanesh, S., Watson, S. J., & Zarouchas, D. (2020). Characterisation of fatigue damage in a thick adhesive joint based on changes in material damping. *Journal of Physics: Conference Series*, *1618*(2), 022058. https://doi.org/10.1088/1742-6596/1618/2/022058

Kumar, A., & Panda, S. (2016). Design of a 1-3 viscoelastic composite layer for improved free/constrained layer passive damping treatment of structural vibration. *Composites Part B: Engineering*, *96*, 204–214. https://doi.org/10.1016/j.compositesb.2016.04.020

Lei, B., Li, J., Wang, J., Peng, G., Fu, B., Zhao, F., & Liao, C. (2024). A novel flexural damping channel magnetorheological damper with high effective magnetic field coverage and experimental verification of damping performance. *Smart Materials and Structures*, *33*(11), 115023. https://doi.org/10.1088/1361-665X/ad8387

Luo, Y., Sun, H., Wang, X., Chen, A., & Zuo, L. (2021). Parametric optimization of electromagnetic tuned inerter damper for structural vibration suppression. *Structural Control and Health Monitoring*, *28*(5), e2711. https://doi.org/10.1002/stc.2711

Meyer, N., & Seifried, R. (2021). Damping prediction of particle dampers for structures under forced vibration using effective fields. *Granular Matter*, *23*(3), 64. https://doi.org/10.1007/s10035-021-01128-z

Mohamed, A., Omer, A. A., & Hassan, A. (2021). Effect of damping material thickness on vibration analysis in pretension layer damping process. *IOP Conference Series: Materials Science and Engineering*, *1172*(1), 012006. https://doi.org/10.1088/1757-899X/1172/1/012006

Nakamura, N., Nabeshima, K., Mogi, Y., & Ota, A. (2024). Nonlinear Earthquake Response Analysis Using Causal Hysteretic Damping and Extended Rayleigh Damping. *Journal of Physics: Conference Series*, *2647*(16), 162004. https://doi.org/10.1088/1742-6596/2647/16/162004

Prayogi, S., Silviana, F., & Saminan, S. (2023). Resistor and Capacitor Time Constant Measuring Instrument Using Arduino UNO. *Jurnal Ilmiah Pendidikan Fisika Al-Biruni*, *12*(1), Article 1. https://doi.org/10.24042/jipfalbiruni.v12i1.15323

Prayogi, S., Silviana, F., & Zainuddin, Z. (2023). Scientific Explanation of the Photoelectric Effect Using Common Objects. *Jurnal Pendidikan Fisika Indonesia*, *19*(2), Article 2. https://doi.org/10.15294/jpfi.v19i2.40332

Rainieri, C., Fabbrocino, G., & Cosenza, E. (2010). Some Remarks on Experimental Estimation of Damping for Seismic Design of Civil Constructions. *Shock and Vibration*, *17*(4–5), 737452. https://doi.org/10.3233/SAV-2010-0534

Silviana, F., & Prayogi, S. (2023). An Easy-to-Use Magnetic Dynamometer for Teaching Newton's Third Law. *Jurnal Pendidikan Fisika Dan Teknologi*, *9*(1), Article 1. https://doi.org/10.29303/jpft.v9i1.4810

Song, R.-F., Wang, J.-L., Yang, Z.-S., & Ma, S.-J. (2025). Optimization Analysis of Vibration Reduction for Large-Span Steel Pedestrian Bridges Based on Tuned Mass Damper Inerter System. *Advances in Civil Engineering*, *2025*(1), 6521700. https://doi.org/10.1155/adce/6521700

Song, X., Cao, T., Gao, P., & Han, Q. (2020). Vibration and damping analysis of cylindrical shell treated with viscoelastic damping materials under elastic boundary conditions via a unified Rayleigh-Ritz method. *International Journal of Mechanical Sciences*, *165*, 105158. https://doi.org/10.1016/j.ijmecsci.2019.105158

Tarpø, M., Georgakis, C., Brandt, A., & Brincker, R. (2021). Experimental determination of structural damping of a full-scale building with and without tuned liquid dampers. *Structural Control and Health Monitoring*, *28*(3), e2676. https://doi.org/10.1002/stc.2676

Wang, L., Nagarajaiah, S., Shi, W., & Zhou, Y. (2020). Study on adaptive-passive eddy current pendulum tuned mass damper for wind-induced vibration control. *The Structural Design of Tall and Special Buildings*, *29*(15), e1793. https://doi.org/10.1002/tal.1793

Wang, W., Hua, X., Chen, Z., Wang, X., & Song, G. (2019). Modeling, simulation, and validation of a pendulum-pounding tuned mass damper for vibration control. *Structural Control and Health Monitoring*, *26*(4), e2326. https://doi.org/10.1002/stc.2326

Wang, W., Hua, X., Wang, X., Wu, J., Sun, H., & Song, G. (2019). Mechanical behavior of magnetorheological dampers after long-term operation in a cable vibration control system. *Structural Control and Health Monitoring*, *26*(1), e2280. https://doi.org/10.1002/stc.2280

Wang, W., Yu, T., Yang, Z., Zhang, H., & Hua, X. (2023). A Double-Tuned Pendulum Mass Damper Employing a Pounding Damping Mechanism for Vibration Control of High-Rise Structures. *Structural Control and Health Monitoring*, *2023*(1), 7686917. https://doi.org/10.1155/2023/7686917

Xiao, J., Wang, C., Wang, C., Ding, T., & Singh, A. (2019). A comparative study on nonlinear damping behaviors of precast and cast-in-situ recycled aggregate concrete frames. *IOP Conference Series: Earth and Environmental Science*, *323*(1), 012135. https://doi.org/10.1088/1755-1315/323/1/012135

Zhang, L., Zhang, L., & Xie, Z. (2022). Hydrodynamic characteristics and application of tuned liquid dampers with internal damping devices. *The Structural Design of Tall and Special Buildings*, *31*(14), e1968. https://doi.org/10.1002/tal.1968

Zhou, X. Q., Yu, D. Y., Shao, X. Y., Zhang, S. Q., & Wang, S. (2016). Research and applications of viscoelastic vibration damping materials: A review. *Composite Structures*, *136*, 460–480. https://doi.org/10.1016/j.compstruct.2015.10.014